

## Isomerization and Hydrogenolysis of C<sub>6</sub> Alkanes on Pt-Al<sub>2</sub>O<sub>3</sub> Catalysts and Pt Single-Crystal Faces

F. GARIN, S. AEIYACH, P. LEGARE, AND G. MAIRE

*Laboratoire de Catalyse et Chimie des Surfaces, ERA 385 du CNRS, Université Louis Pasteur, 67000 Strasbourg, France*

Received April 16, 1981; revised May 4, 1982

The contact reactions of C<sub>6</sub> hydrocarbons (isomerization, dehydrocyclization, hydrocracking) were studied under the same experimental conditions, on platinum-alumina catalysts of low or high dispersion, on Pt(557), Pt(119), Pt(111) surfaces, and on a polycrystalline foil of platinum. The experiments on these well-characterized surfaces were performed up to atmospheric pressure in an isolation cell housed within the main UHV chamber equipped with LEED, AES, and ELS facilities. The reaction mixture was analyzed by GLC and part of it was used for mass spectrometric location of the <sup>13</sup>C in each molecule. The results have shown that isomerization by bond-shift or cyclic mechanisms and hydrogenolysis take place on single-crystal faces of platinum, simulating very well the data from Pt-Al<sub>2</sub>O<sub>3</sub> catalysts of large size aggregates of Pt. Isomerization by bond shift is much more important on stepped surfaces. The contributions of the relative percentages of bond-shift and cyclic mechanisms are discussed as a function of different models of adsorbed species evolving from one site to multisites of chemisorption, differences in local density of states of the edges, and differences in the electronic charges of the carbon atoms in the hydrocarbons. These models are correlated to the classical ones of Anderson, Rooney, and Gault. The peculiar properties of the highly dispersed 0.2% Pt-Al<sub>2</sub>O<sub>3</sub> catalyst were never simulated by single crystals of platinum.

### I. INTRODUCTION

Studies of the isomerization of labeled hydrocarbons on supported polycrystalline catalysts or on films, deposited on glass, allowed us to characterize the different skeletal reaction mechanisms, bond-shift (1) and cyclic mechanisms (2), which occur on metal particles, and to evaluate roughly their relative amounts with metal particle size as a parameter (3). However, it has not yet been possible to define and characterize the real nature of the active catalytic sites associated with each reaction pathway other than by indirect, often speculative arguments. It was the aim of this study, using well-defined surfaces of platinum single crystals of both low and high index, to find a possible correlation between crystallographic arrangements and these catalytic skeletal reactions.

Surfaces with well-defined and well-characterized defects, such as steps and kinks,

have been used in a series of earlier catalytic studies by Lang, Joyner, and Somorjai (4, 5, 8, 13) and more recently by Somorjai and co-workers (6a,b). Their major conclusions were concerned with the dehydrocyclization of *n*-heptane and the dehydrogenation of cyclohexane which are mainly favored by low-coordinated atoms (kinks or step atoms). The selectivity for cyclization of *n*-heptane is highest on the (557) and (10, 8, 7) surfaces (6) and lower on the (111) and on the (25, 10, 7) surfaces. The (111) surface possesses no steps while the (25, 10, 7) surface has closely spaced steps. The authors (6b) concluded from their results that steps separated by six- to seven-atom-wide terraces, or the combination of a step and a six- to seven-atom-wide terrace, are structures that favor the dehydrocyclization of *n*-heptane. Otherwise multiple attachment of *n*-heptane may hinder cyclization and enhance hydrogenolysis on closely spaced steps. Unfortunately

these studies were monitored with a reaction such as the dehydrocyclization of *n*-heptane, the mechanisms of which are complex as shown by tracer studies on platinum–alumina catalysts (7, 9). Moreover Somorjai and co-workers did not consider reaction pathways such as isomerization and cyclization to five-membered rings.

The hydrogenolysis of methylcyclopentane and the isomerization of  $^{13}\text{C}$ -labeled hexanes were studied on Pt(557), Pt(119), Pt(111) single crystals, a Pt polycrystalline foil, and four supported platinum–alumina catalysts with a metal dispersion extending from 4 to 100%. The thermal stability of ordered stepped surfaces indicates that they are likely to be present on metal particles which are commonly used as catalysts for surface chemical reactions (4, 5).

## II. EXPERIMENTAL

### *Materials*

The synthesis of most of the  $^{13}\text{C}$ -labeled hydrocarbons used as reactants or references for mass spectrometry has been described (11). The unlabeled hydrocarbons were Fluka puriss grade. Before each experiment the reacting hydrocarbon was purified by gas–liquid chromatography and correct labeling ascertained by mass spectrometry.

### *Apparatus and Procedure*

*Catalytic experiments on single crystals.* The experiments were performed in a Varian LEED chamber with 4-grid optics. The Auger detector used to monitor the surface composition was a retarding field analyzer (referred to as RFA). The energy of primary electrons was about 2 kV and they struck the sample at normal incidence. The beam current was about 20  $\mu\text{A}$ . A 140-liter/sec ion pump and a titanium sublimation pump allowed us to reach ultimate pressures in the low  $10^{-10}$  Torr range after baking (Fig. 1). An isolation cell housed within the main UHV chamber allowed catalytic

reactions up to atmospheric pressure with the rest of the chamber remaining in ultra-high vacuum. The "high-pressure reaction vessel" was connected to a gas inlet system. Crystal samples could be heated during low- and high-pressure experiments up to at least 1200°C as described elsewhere (18, 19, 26). The crystal samples were mounted on tantalum rods and heated by direct Joule effect. A chromel–alumel thermocouple was spotwelded on the single-crystal slices. The temperature of the samples given by the thermocouple ( $\pm 5^\circ\text{C}$ ) was compared to the data given by an Ircon photometer in the range 200–1200°C in UHV. No gradient of temperature was detected over all the single crystals in that range. The catalytic properties of the tantalum crystal holder were undetectable as tested by blank experiments for hydrogenolysis and isomerization of hexanes under the same experimental conditions, which means no background reactivity due to the sample mounting. Furthermore, great care was taken to do all the experiments on single crystals at the *same temperature* from one sample to another ( $350 \pm 5^\circ\text{C}$ ). Each experiment was done under standard experimental conditions. In each run 5 Torr of hydrocarbon was introduced with 755 Torr of pure hydrogen (air liquid 99.99% N). After 1 hr contact time for a well-controlled temperature the reaction products were trapped in liquid nitrogen. A fraction of the gas phase was directly analyzed by gas chromatography over an alumina column to obtain a quantitative measurement of  $\text{CH}_4$  versus  $\text{C}_2\text{H}_6$  formed during the reaction. The reaction mixture was then analyzed by chromatography and a part of it was used for mass-spectrometrical location of the  $^{13}\text{C}$  in each molecule. These experiments done on single crystals were highly reproducible for both activity and selectivity provided the initial cleanliness of the surface was suitable as ascertained by AES and ELS spectroscopies. One example is given in Table 1 for the isomerization of 2-methylpentane at 350°C,  $P_{\text{H}_2} = 755$  Torr and  $P_{2\text{MP}}$

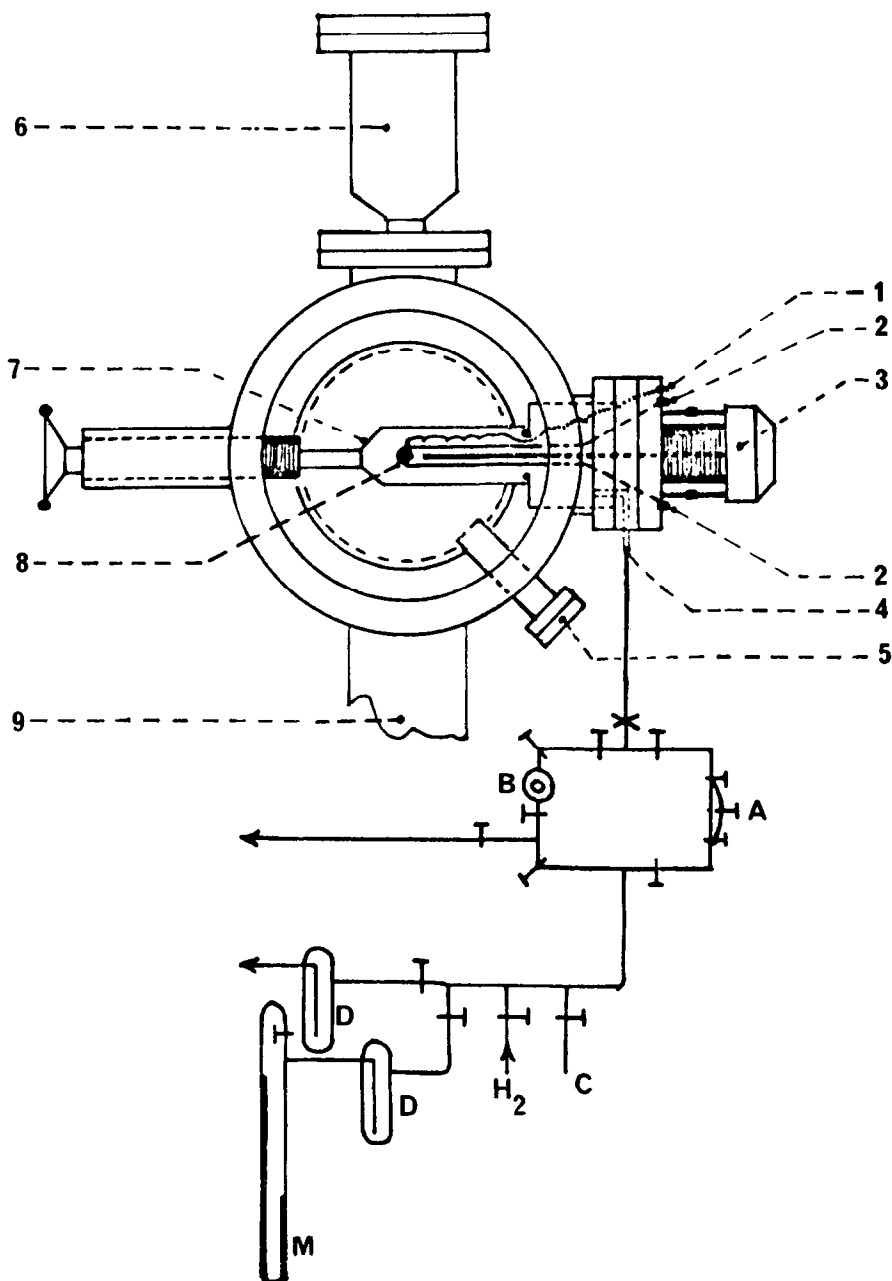

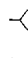

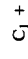
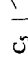
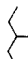


FIG. 1. Schematic of UHV assembly and gas inlet system for high-pressure (1 atm) catalysis on single-crystal platinum surfaces. (1) chromel–alumel thermocouple, (2) sample heating by direct Joule effect, (3) sample manipulator, (4) to gas manifold, (5) ion gun, (6) quadrupole mass analyzer, (7) sample isolation cell, (8) platinum sample mounted on tantalum rods, (9) to UHV gate valve, (x) metallic valve, (T) Teflon-sealed valve, (A) hydrocarbon loop, B, reaction products trapped in LN, (C) to thermocouple gauge, (D) LN traps, (M) Hg manometer.

TABLE I  
Isomerization of 2-Methylpentane at 350°C<sup>a</sup>

Catalyst	$\alpha =$ H/Pt	% <sub>cat</sub> (moles) <sup>b</sup>	% $S_T$ (isom) <sup>c</sup>	6C <sub>1</sub>	3C <sub>2</sub>	C <sub>1</sub> + C <sub>5</sub>	C <sub>2</sub> + C <sub>4</sub>	2C <sub>3</sub>			$\frac{C_1 + C_5}{C_2 + C_4}$					
Pt-Al <sub>2</sub> O <sub>3</sub> , 10%	0.04	0.9	76.2	0	0	10.8	6.8	5.5	20.0	15.6	40.6	0	1.60	1.30	1.95	12.40
Pt-Al <sub>2</sub> O <sub>3</sub> , 2%	0.05	2.8	94.5	0	0	1.5	2.3	1.6	28.5	12.9	53.1	0	0.65	2.20	1.75	7.00
Pt-Al <sub>2</sub> O <sub>3</sub> , 5%	0.2	2.8	94.2	0	0	1.9	2.1	1.8	31.0	16.5	46.7	0	0.90	1.90	1.65	5.00
Pt-Al <sub>2</sub> O <sub>3</sub> , 0.2%	1	3.4	92.7	0	0	3.8	1.9	1.4	14.1	35.2	42.9	0.5	2.00	0.40	1.85	10.00
Pt(557)		0.85	72.1	2.8	0.5	7.1	10.2	7.1	19.7	9.5	42.9	0	0.70	2.10	2.00	13.30
Pt(557) <sup>d</sup>		0.90	73.9	—	—	—	—	—	24.4	9.9	39.6	0	—	2.46	—	—
Pt(111)		0.2	53.5	—	—	—	—	—	5.5	3.5	43.0	1.5	—	1.60	1.70	2.55
Pt(119)		0.5	43.2	1.6	0	11.6	25.5	17.9	5.3	5.1	28.0	4.8	0.45	1.05	1.65	5.55
Pt polycrystalline		3.2	69.9	0.7	1.3	5.9	11.9	10.3	15.4	11.0	43.4	$\epsilon$	0.50	1.40	1.45	5.0

<sup>a</sup>  $p_{H_2} = 755$  Torr and  $p_{HC} = 5$  Torr.

<sup>b</sup> %<sub>cat</sub>(moles) = overall conversion.

<sup>c</sup>  $S_T$ (isom) = selectivity defined as the percentage (in moles) of C<sub>6</sub> isomers in the reaction products.

<sup>d</sup> Quantification of the reproducibility and activity %<sub>cat</sub>  $\pm$  0.1; % $S_T$ (isom)  $\pm$  2.

= 5 Torr. All the conversions in isomerization and hydrogenolysis are given for a 1-cm<sup>2</sup> area of platinum.

### Cleaning and Preparation of Single-Crystal Surfaces

The three types of platinum single-crystal surfaces studied—Pt(557), Pt(119), and Pt(111)—were cut from the same single-crystal rod (MRC, purity 99.999%) by spark erosion after orientation with Laue back-reflection techniques ( $\Delta\theta = \pm 15$  min). The slices obtained were 0.5 mm thick and 1 cm<sup>2</sup> in area on both sides. The polished Pt surfaces were cleaned as described elsewhere (18, 27) until AES spectra revealed a minimum of impurities (C, S, Ca, Al, Si, and P being the usual impurities). For both (557) and (119) stepped surfaces after cleaning and annealing, monoatomic steps were formed in agreement with LEED patterns (4, 18). The mean terrace width calculated from the doublet separation of the 00 beam agreed well with the theoretical one (18). A Pt polycrystalline surface was also studied during the course of this work. The cleaning procedure of the polycrystalline foil was the same as for the single crystal, i.e., heating the foil, a  $1 \times 1.5 \times 0.02$ -cm Pt sheet of 99.9% purity, to temperatures not exceeding 700°C in oxygen. The samples were judged clean when the ratios of the peak-to-peak height, given by AES, were:  $h(\text{Pt} + \text{S})/h(\text{Pt})$  167 eV  $\leq$  0.85;  $h(\text{C})/h(\text{Pt})$  269 eV  $\leq$  0.01;  $h(\text{Ca})/h(\text{Pt})$  290 eV  $\leq$  0.02;  $h(\text{P})/h(\text{Pt})$  115 eV  $\leq$  0.02. No surface impurities (i.e., Cl, O, P) were detected following the reactions. Some traces of sulfur ( $\theta \leq 0.25$ ) could sometimes be detected after reactions under H<sub>2</sub> pressure (1 atm).

*Experiments on supported catalysts.* The differential reactor and the experimental procedure for catalytic experiments at atmospheric hydrogen pressure on supported catalysts have been described elsewhere (11, 12). In each run a very small amount of labeled hydrocarbon (ca. 4 mg) was passed over the catalyst at constant pressure (2-

methylpentane, 3.9 Torr; 3-methylpentane, 2.9 Torr). In each run a part of the reaction mixture was analyzed by chromatography over a 5-m ×  $\frac{1}{8}$ -in. column of DC 200/fire brick and a part was used for mass-spectrometrical location of the label in each molecule using a GLC–MS system. Four Pt–Al<sub>2</sub>O<sub>3</sub> catalysts were prepared by impregnating inert WOELM alumina with a chloroplatinic solution. In all cases the reduction was carried out at 200°C for 48 hr with a hydrogen flow rate of 10 ml·min<sup>-1</sup>. An industrial 5% Pt–Al<sub>2</sub>O<sub>3</sub> catalyst, interesting for its narrow particle size distribution (3a) (around 30 Å), was purchased from Matheson–Coleman.

### III. RESULTS

#### 1. LEED and Auger Spectroscopy Data

The first important result which will be discussed is the phenomenon of terrace broadening induced by hydrogen that occurred during reactions in the presence of hydrocarbon for Pt(557) alone as described elsewhere (18a,b, 19). Reconstruction of Pt(557) under atmospheric pressure of hydrogen at 350°C led to diffraction features strictly identical to those published in Ref. (18). The intradoublet separation which is dependent on the distance between steps (i.e., the terrace width) was changed and corresponded to a terrace width of  $2(5 + \frac{2}{3})$  (number of periods). No extra faceting was observed on the LEED patterns due to multiple height steps and low index facets. The reversibility of the change-of-step configuration by heating at 700°C in UHV implies also a surface reconstruction rather than faceting. Surprisingly the carbonaceous overlayer deposited by the reaction mixture could be almost removed by heating in UHV to 700°C, i.e., the ratio  $c = h(C) 270 \text{ eV}/h(\text{Pt}) 233 \text{ eV}$  given by Auger spectroscopy dropped from 0.9 after isomerization of 2-methylpentane to less than 0.08. Furthermore no graphitic rings were observed on the LEED patterns of the Pt(557). When Pt(111) or Pt(119) was heated after reac-

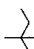

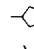

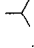
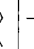

tions in UHV above 500°C, a ring appeared with 12 reinforcements corresponding to domains of graphite (0001) (27). When the carbonaceous overlayer deposited after reaction on Pt(119) was heated to 700°C, faceting of Pt(100) took place. The facets giving the most intense specular reflections are (113) and (115) faces. In view of these results the Pt(557) stepped surface thus reacted with the reaction mixture ( $p\text{H}_2/p\text{HC} = 150$ ) in a manner which was similar to exposure at hydrogen alone provided the temperature was high enough (350°C) and in a manner which was different from that observed on Pt(111) and Pt(119). Lang, Joyner, and Somorjai (4, 8) came to the conclusion that hydrogen dissociates more easily on surface with (111) or (100) steps. In our experiments we believe that the hydrogen atoms penetrate into the crystal lattice on stepped and low index faces of platinum and induce a change-of-step configuration for Pt(557). The same features were recently observed in our laboratory (18) for Pt(69,72,72) and Pt(4,5,6) but never for Pt(119) or Pt(799).

#### 2. Hydrogenolysis of 2- and 3-Methylpentanes

The product distributions for hydrogen, obtained at 350°C under 760 mm Hg on four supported catalysts, three single crystals, and a polycrystalline foil, are shown in Tables 1 and 2, where  $\% \alpha_T$  (moles) is the overall conversion and  $\% S$  (isom.) is the selectivity defined as the percentage (in moles) of C<sub>6</sub> isomers in the reaction products. Consecutive reactions were always negligible as shown by the high isobutane/*n*-butane and *n*-butane/isobutane ratios, obtained from 2- and 3-methylpentanes, respectively, and the small amount of propane obtained from 3-methylpentane.

In order to make a distinction between the various catalysts we examined the ratio  $R_3 = 3\text{-methylpentane}/n\text{-hexane}$ , obtained from the isomerization of 2-methylpentane, on Pt(557), Pt(119), Pt(111), and Pt polycrystalline foil, and the ratio  $R_2 = 2\text{-methyl}$

TABLE 2  
Isomerization of 3-Methylpentane at 350°C<sup>a</sup>

Catalyst	a = H/PT	% $\alpha_1$ (moles) <sup>b</sup>	% $S_1$ (isom) <sup>c</sup>	6C <sub>1</sub>	3C <sub>2</sub>	C <sub>1</sub> + C <sub>3</sub>	C <sub>2</sub> + C <sub>4</sub>	2C <sub>3</sub>					$\frac{C_2 + C_5}{C_3 + C_4}$				
Pt-Al <sub>2</sub> O <sub>3</sub> , 10%	0.04	3.4	88.3	0	0	7.2	4.1	0.4	1.0	51.3	18.6	17.4	0	1.75	2.75	0.30	10
Pt-Al <sub>2</sub> O <sub>3</sub> , 2%	0.05	3.3	94.4	0	0	2.4	2.8	0.2	0.9	54.7	12.7	26.1	0	0.85	4.30	0.25	10
Pt-Al <sub>2</sub> O <sub>3</sub> , 5%	0.2	2.8	95.2	0	0	2.2	2.5	0.2	1.4	61.8	12.1	20.0	0	0.90	5.15	0.25	10
Pt-Al <sub>2</sub> O <sub>3</sub> , 0.2%	1	3.4	92.1	0	0	5.3	2.5	0.1	0.4	44.6	21.9	25.2	0	2.10	2.05	0.35	25
Pt(557)		0.62	76.2	1.0	1.4	11.4	9.4	1.4	2.0	29.9	10.6	33.7	0	1.20	2.80	0.20	17
Pt(111)		0.65	16.3	8.1	0	36.4	33.5	5.6	0.2	3.8	1.5	9.9	0.9	1.10	2.50	0.20	17
Pt polycrystalline		3.4	56	0	0	12.4	17.8	4.8	0.4	15.4	8.1	38.5	2.5	0.7	1.90	0.45	5

<sup>a</sup> p<sub>H<sub>2</sub></sub> = 755 Torr and p<sub>HC</sub> = 5 Torr.

<sup>b</sup> % $\alpha_1$ (moles) = overall conversion.

<sup>c</sup> S (isom) = selectivity defined as in Table 1.

pentane/*n*-hexane from the isomerization of 3-methylpentane; in addition to the normal isomerization and hydrogenolysis reactions we observed a small extensive cracking corresponding roughly to 3% of the products.

Pt(557) gave the same ratio  $R_3$  as the 2 and 5% Pt-Al<sub>2</sub>O<sub>3</sub> catalysts. The percentage of cracking and the ratio  $R_2$  looked like those obtained on 10% Pt-Al<sub>2</sub>O<sub>3</sub>. It is worthwhile to note the high selectivity given by this surface compared to the other single crystals and the polycrystalline surface.

Pt(119) gave a ratio  $R_3$  equivalent to the 10% Pt-Al<sub>2</sub>O<sub>3</sub>. The selectivity in isomerization was lower than those obtained on supported catalysts.


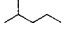
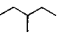
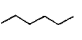
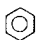
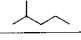
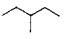
Pt(111) gave  $R_3$  ratio between the two values obtained on the stepped faces. The ratio *n*-pentane/isopentane was the same as for the Pt-Al<sub>2</sub>O<sub>3</sub> catalysts. In that case we detected the presence of benzene. On the polycrystalline foil (111) terraces predominated which resulted in a selectivity for both 2- and 3-methylpentanes isomerization similar to those given by (557) Pt plane. The ratio  $R_3$  was comparable to the values obtained on low dispersed catalysts. A small deviation was noted for the amounts of methylcyclopentane and *n*-hexane formed by isomerization of 3-methylpentane.

### 3. Hydrogenolysis of Methylcyclopentane

The results obtained at 350°C under atmospheric hydrogen pressure are mentioned in Table 3. On the supported catalysts, no hydrocracking reaction was observed. The 0.2% Pt-Al<sub>2</sub>O<sub>3</sub> catalyst was the only one to give an equal rupture between the CH<sub>2</sub>-CH<sub>2</sub> and CH<sub>2</sub>-CH bonds of the ring. The ratio 2-methylpentane/3-methylpentane was practically constant whatever the catalyst used.

On single crystals and on the polycrystalline surface we observed some extensive cracking reactions and especially on the Pt(111). On the other hand the 3-methylpentane/*n*-hexane ratio showed that single

TABLE 3  
 Hydrogenolysis of Methylcyclopentane<sup>a</sup>

Catalysts	% $\alpha_T$ (moles)	% $\Sigma$ (acyclic cracking)							
Pt(111)	0.3	40.3	3.3 <sup>b</sup>	34.7	17.4	5.9	1.6	2.0	2.95
Pt(557)	2.8	3.2	0	58.3	21.6	14.5	2.3	2.7	1.50
Pt polycrystalline	5.0	6.9	0	50.9	23.4	18.4	0.4	2.2	1.30
Pt–Al <sub>2</sub> O <sub>3</sub> , 10%	3.8	1.5	1.4	47.6	20.5	20.2	8.6	2.3	1.0
Pt–Al <sub>2</sub> O <sub>3</sub> , 2%	6.5	0	0	65.4	21.9	8.5	4.1	3.0	2.6
Pt–Al <sub>2</sub> O <sub>3</sub> , 5%	10.0	0	0	66.4	21.0	11.4	1.1	3.2	1.8
Pt–Al <sub>2</sub> O <sub>3</sub> , 0.2%	5.8	0	0	48.4	16.6	30.3	4.7	2.9	0.55

<sup>a</sup> Product distributions at 350°C;  $p_{H_2} = 755$  Torr;  $p_{HC} = 5$  Torr. % $\alpha_T$ (moles) = overall conversion.

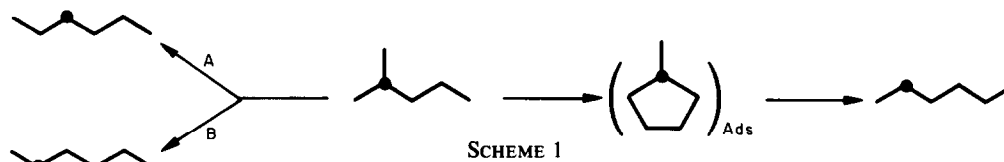
<sup>b</sup> Values are percentages.

crystals and polycrystalline surfaces behave as low dispersed catalysts. We could notice a small amount of benzene on supported catalysts which decreased on single crystals.

#### 4. Isomerization of Labeled C<sub>6</sub> Hydrocarbons

The isomerization of 2-[2-<sup>13</sup>C]methylpentane, 2-[4-<sup>13</sup>C]methylpentane, and 3-[3-

<sup>13</sup>C]methylpentane has been studied at 350°C under 1 atm of H<sub>2</sub> on supported catalysts, single crystals, and a polycrystalline foil. In Tables 4 and 5 we report the distributions of the observed isotopic varieties and the percentages of the cyclic and bond-shift mechanisms. The amount of *n*-[3-<sup>13</sup>C]hexane obtained in the isomerization of 2-[2-<sup>13</sup>C]methylpentane allowed us to determine the percentage of bond-shift A mechanisms (Scheme 1).



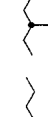




*Isomerization of 2-methylpentane to 3-methylpentane.* The isotopic distributions for the labeled 3-methylpentanes are mentioned in Table 4. The percentages of the cyclic mechanism on the low dispersed catalysts were about 30 to 35%. We give for reference a catalytic result obtained on a highly dispersed catalyst (0.2% Pt–Al<sub>2</sub>O<sub>3</sub>) at 254°C. At this temperature the cyclic mechanism is already important and we know that it increases with the temperature (12) which is noticeable in Table 4 for an experiment performed at 254°C on the 5% Pt–Al<sub>2</sub>O<sub>3</sub>. On the stepped face Pt(557) the percentage of cyclic mechanism was lower than on low dispersed catalysts. On the

other hand the percentage of cyclic mechanism was higher on Pt(119) than on the supported catalysts with low dispersion. The polycrystalline surface led surprisingly to ~50% of cyclic mechanism.

*Isomerization of 2-methylpentane to *n*-hexane.* The percentage of cyclic mechanism (Table 4) was the same on Pt(557) as on the low dispersed Pt–Al<sub>2</sub>O<sub>3</sub> catalysts and was greatly different from the data obtained on 0.2% Pt–Al<sub>2</sub>O<sub>3</sub>. The percentage of the bond-shift A compared to the bond-shift B was higher on the stepped faces than on the supported catalysts at 350°C under 1 atm of H<sub>2</sub>. On the polycrystalline surface the percentage of cyclic mechanism was

TABLE 4  
Isomerization of 2-[2-<sup>13</sup>C]MP, 2-[4-<sup>13</sup>C]MP, and 3-[3-<sup>13</sup>C]MP at 350°C<sup>a</sup>

Catalysts	<i>a</i> = H/Pt	Percentage cyclic mechanism			Percentage bond-shift mechanism	
					Mode A 	Mode B <sup>b</sup> 
Pt(S57)		13.5	70.4	50.5	20.5	9.1
Pt(119)		39	—	—	30	—
Pt polycrystalline		49	65	64	13.3	21.7
Pt-Al <sub>2</sub> O <sub>3</sub> , 5%	0.2	34	71.6	61	10	18.4
Pt-Al <sub>2</sub> O <sub>3</sub> , 5% [254°C, Ref. (3)]	0.2	7	52	49	10	38
Pt-Al <sub>2</sub> O <sub>3</sub> , 2%	0.05	30	64.4	55	10.3	25.3
Pt-Al <sub>2</sub> O <sub>3</sub> , 0.2% [254°C, Ref. (3)]	1	83	100	95	0	0

<sup>a</sup> *p*H<sub>2</sub> = 1 atm.

<sup>b</sup> Percentage bond-shift mechanism (Mode B) = 100 - %  - %  - %  - % BSA.



comparable to the values obtained on large size Pt–Al<sub>2</sub>O<sub>3</sub> catalysts.

*Isomerization of 3-methylpentane to n-hexane.* The percentages of the cyclic mechanism (Table 4) were 55 and 61% on the two low dispersed catalysts; on the Pt(557) we obtained 50.5 and 64% on the polycrystalline surface.

#### IV. DISCUSSION

From these results it appears that the well-characterized Pt surfaces and the Pt polycrystalline foil have catalytic behavior quite similar to that of the large-size Pt–Al<sub>2</sub>O<sub>3</sub> catalysts, the predominant mechanism being bond shift for the reaction 2-methylpentane → 3-methylpentane, while on high-dispersed catalysts (0.2% Pt–Al<sub>2</sub>O<sub>3</sub>) both selective and nonselective cyclic mechanisms at as low a temperature as 254°C predominate. This clearly indicates that the small metal aggregates on high dispersed platinum catalysts do not exhibit metallic properties any more. This important result confirms the hypothesis that the metal aggregates in these catalysts are no longer fcc crystals (15) but small clusters with uncommon symmetry (i.e., icosahedral) as proposed by Burton (16) or small clusters of normal symmetry according to Hoare and Pal (17). The small clus-

ters on high dispersed Pt–Al<sub>2</sub>O<sub>3</sub> catalysts may rather be considered as molecular particles having electronic properties that differ from the ones in the infinite crystals.

Under constant reaction conditions, the reactivity and the selectivity change significantly as a function of the structure of the well-characterized Pt surfaces. Examination of the data in Tables 1–4 reveals that the activity the selectivity and the percentage of bond-shift mechanisms are more significant for the (557) surface. The hydrocracking in small molecules is much more important on the (111) face than on the stepped surface or on the Pt–Al<sub>2</sub>O<sub>3</sub> catalysts (Table 3). For hydrogenolysis of methylcyclopentane and isomerization of hexanes which are structure sensitive reactions (3b) we have the classifications reported in Table 5. These classifications are corroborated by those of Gillespie *et al.* (6b) for cyclization and hydrogenolysis of *n*-heptane on the Pt(557), Pt(10,8,7), Pt(25,10,7), and Pt(111) surfaces. The location of the Pt polycrystalline foil between the Pt(557) and the Pt(111) faces is due to the existence of fairly good single-crystal grains of (111) orientation detected by LEED giving well-defined diffraction spots of threefold symmetry. The high activity of the Pt polycrystalline foil is attributed to the high density of defects. But the Pt(111) low index face is not totally inactive as it is shown in Tables 1–3. The following statement arises: the total activity for hexane conversion is not linked to the density of steps whereas the amount of the cracking reaction (i.e., reaction of 2-methylpentane) seems directly proportional to the density of defects as seen in Table 6 where we reported: the total conversion % $\alpha_T$ ; the total cracked products; the acyclic and cyclic molecules formed via a cyclic mechanism; the sum of these molecules  $\Sigma CM$ ; the total density of defects taking into account the thickness of the crystal slices by supposing a quasi-identical repartition between (111) and (100) ledges. The defects due to the thickness of the slice did not affect very

TABLE 5

Effect of Platinum Surface Structure on the Selectivity in Hydrogenolysis of MCP, Selectivity in Isomerization, and the Ratio  $\Sigma CM/\Sigma BS$

Platinum surface	(557)	Polycrystalline foil	(119)	(111)
Selectivity for hydrogenolysis of MCP	94.5%	92.7%	—	58.1%
Selectivity for isomerization				
2-MP	73%	70%	43.2%	53.5%
3-MP	76%	56%	—	16.3%
$\Sigma CM/\Sigma BS$ for isomerization of 2-MP <sup>a</sup>	2.6	5.7	8.5	9

<sup>a</sup> On Pt(111),  $\alpha_T$  being very low;  $\Sigma CM/\Sigma BS \sim [MCP]/\Sigma BS$ ;  $\Sigma CM = \Sigma$ acyclic C<sub>6</sub> formed via CM + MCP;  $\Sigma BS = \Sigma$ acyclic C<sub>6</sub> formed via BS.

TABLE 6  
Product Distribution for 100 moles of 2-Methylpentane Initial on Various Catalysts at 350°C<sup>a</sup>

Catalyst	%α <sub>T</sub> (moles)	Percentage cracking	Molecules formed via cyclic mechanism			%ΣCM	%ΣBS	Total density of defects
			3-MP	<i>n</i> -H	MCP			
Pt polycrystalline	1.7	0.6	0.099	0.114	0.717	0.93	0.164	
Pt(557)	0.85	0.235	0.023	0.057	0.365	0.445	0.170	0.22
Pt(119)	0.5	0.285	0.010	0.017	0.165	0.192	0.023	0.27
Pt(111)	0.2	0.090	0.0035	0.0045	0.090	0.099	0.011	0.09
Pt(557) (450°C, 12 Torr H <sub>2</sub> )	1.7	0.243	0.017	0.017	1.368	1.403	0.042	0.22

<sup>a</sup>  $p_{H_2} = p$  atm.  $\% \alpha_T = \% \text{ cracking} + \% \Sigma \text{CM} + \% \Sigma \text{BS} = \text{overall conversion}$ .

much the selectivity and the total activity of the three single crystals studied. The experiment on Pt(557) at low pressure of hydrogen (12 Torr) confirms this fairly rough hypothesis (Table 6). The amount of cracked molecules for 100 starting molecules is the same whatever the experimental conditions. The cyclic products are the only ones desorbed (9).

But checking carefully the behavior for isomerization given by the Pt(557) plane the question arises, why is the bond-shift

mechanism more significant than on Pt(119) or Pt(111) faces? The ratio  $\Sigma \text{CM} / \Sigma \text{BS}$  varies from 2.6 for Pt(557) to 8.5 for Pt(119) and reaches 9 for Pt(111) (Table 5). For this particular type of isomerization via a bond-shift mechanism it is clear that the structure of the Pt surface seems directly responsible for the increase of bond shift. Four basic mechanisms have so far been proposed for bond-shift isomerization (1-3, 12). On account of the complexity of the carbon-metal bonding in these intermediates, besides

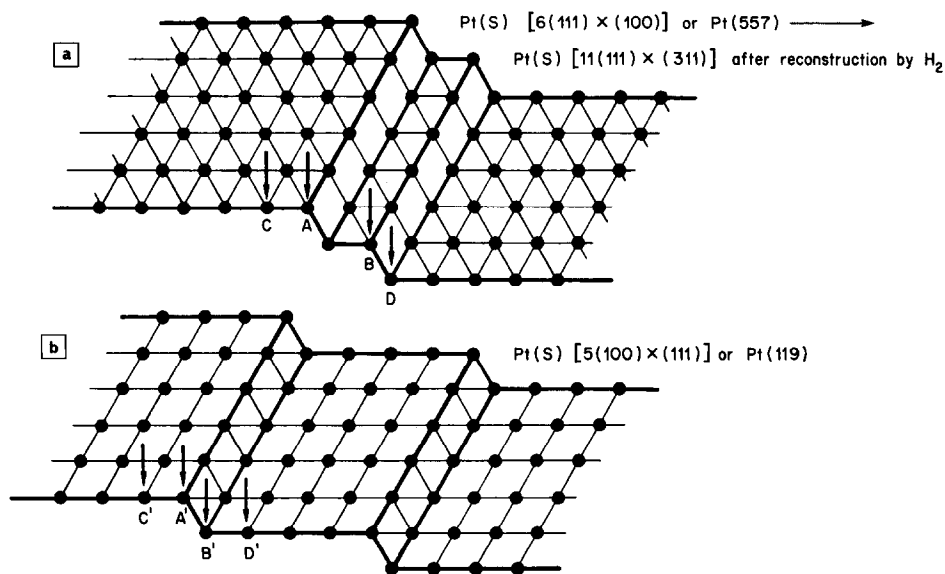


FIG. 2. Representation of the different edges for the (a) Pt(557) and (b) Pt(119) stepped surfaces. Hypothesis A:  $n(E)_A \neq n(E)_B \neq n(E)_C \neq n(E)_D$ . Hypothesis B:  $n(E)_{A'} \neq n(E)_{B'} \neq n(E)_{C'} \neq n(E)_{D'}$ .

the steric requirements according to which some reactions involve several metal atoms and some only one (31), the local electronic density around a surface metal atom should widely influence the relative stabilities and reactivities of the various precursor and transient species. Taking into account the experimental and theoretical works done on stepped surfaces of platinum (21–25), we attributed the increase of the bond shift on the Pt(557) to the conjugate electronic properties of the surface atoms and to the electron density in alkanes (32). Our explanation is based on a surface reconstruction approach (18, 19). The reconstruction of the Pt(557) surface under atmospheric pressure of H<sub>2</sub> at 350°C giving (113) ledges or (113) B<sub>2</sub>' sites according to the model that we proposed to explain the step coalescence (18a, 19) may explain the catalytic experimental data. On the Pt(557) and Pt(119) surfaces (Fig. 2), the Pt atoms located on the edges belong to the (113) B<sub>2</sub>' sites (28). If one attributes the bond-shift mechanism to these edge atoms, no drastic difference should occur for the  $\Sigma\text{CM}/\Sigma\text{BS}$  ratio on both stepped surfaces. We postulate that the change in the geometry of the ledges added to the presence of hydrogen along the edges (25) can greatly modify the local density of states on the edges A and B in Fig. 2a and, but not in the same way, on the edges A' and B' in Fig. 2b; we believe that more than one single metal atom must operate in the bond-shift isomerizations. Figures 3 and 4 show models of precursor species with the different atoms involved either in the reaction of a chain lengthening or for the methyl shift via a bond shift type A and B (3). In such models we assume that multiadsorbed species are formed as precursors on at least two atoms in agreement with both mechanisms of Gault and Anderson (1, 2). By the way the distance between the two carbon atoms 1 and 3 fits nicely with the unit mesh of the (113) plane (Fig. 3). Furthermore when no reconstruction by hydrogen of Pt(557) occurred as seen by LEED, we obtained *exactly* the same distri-

butions of products in the isomerization for neopentane (9) on Pt(111) which proves the role of the reconstruction by hydrogen and especially of the nature of the ledges. It is worthwhile to emphasize the fact that Pt(557) presents strictly the same catalytic behavior for isomerization and hydrogenolysis as Pt–Al<sub>2</sub>O<sub>3</sub> catalysts with large-size aggregates (Tables 1, 2, 3, and 4). It is well known (16) that for large-size Pt aggregates (around 100 to 200 Å) B<sub>2</sub>' and B<sub>2</sub>' sites arise by addition of incomplete layers adsorbed on (111) and (100) faces of fcc crystals. We know that these hypotheses are highly speculative but the proposed model of Pt(557) reconstruction accounts for experimental data and therefore seems reasonable. In addition the proposed models of Figs. 3 and 4 have the advantage of giving an explanation to the experimental data reported in Table 4, namely, the increase of bond shift A in chain lengthening mechanism: 20.5 and 30% on Pt(557) and Pt(119), respectively. As for the Pt(557) surface we consider that the nearest atomic row (C') and the edge (A') (Fig. 2b) are cooperating together with their own local density of states to the bonding of the hydrogen. On another hand Gillespie *et al.* (6b) obtained peculiar results on Pt(557) for cyclization of *n*-heptane. These authors came to the conclusion that steps separated by six- to seven-atom-wide terraces, or the combination of a step and a six- to seven-atom-wide terrace is a structure that favors cyclization of *n*-heptane. Our assumption of surface reconstruction producing a new type of active site selective for bond-shift isomerization would fit also the results of Gillespie *et al.* (6b).

#### CONCLUSION

The low or high index faces of platinum simulate very well the supported catalysts with low dispersion (large-size aggregates). The peculiar properties of the highly dispersed 0.2% Pt catalyst with metal particles smaller than 10 Å are never simulated by

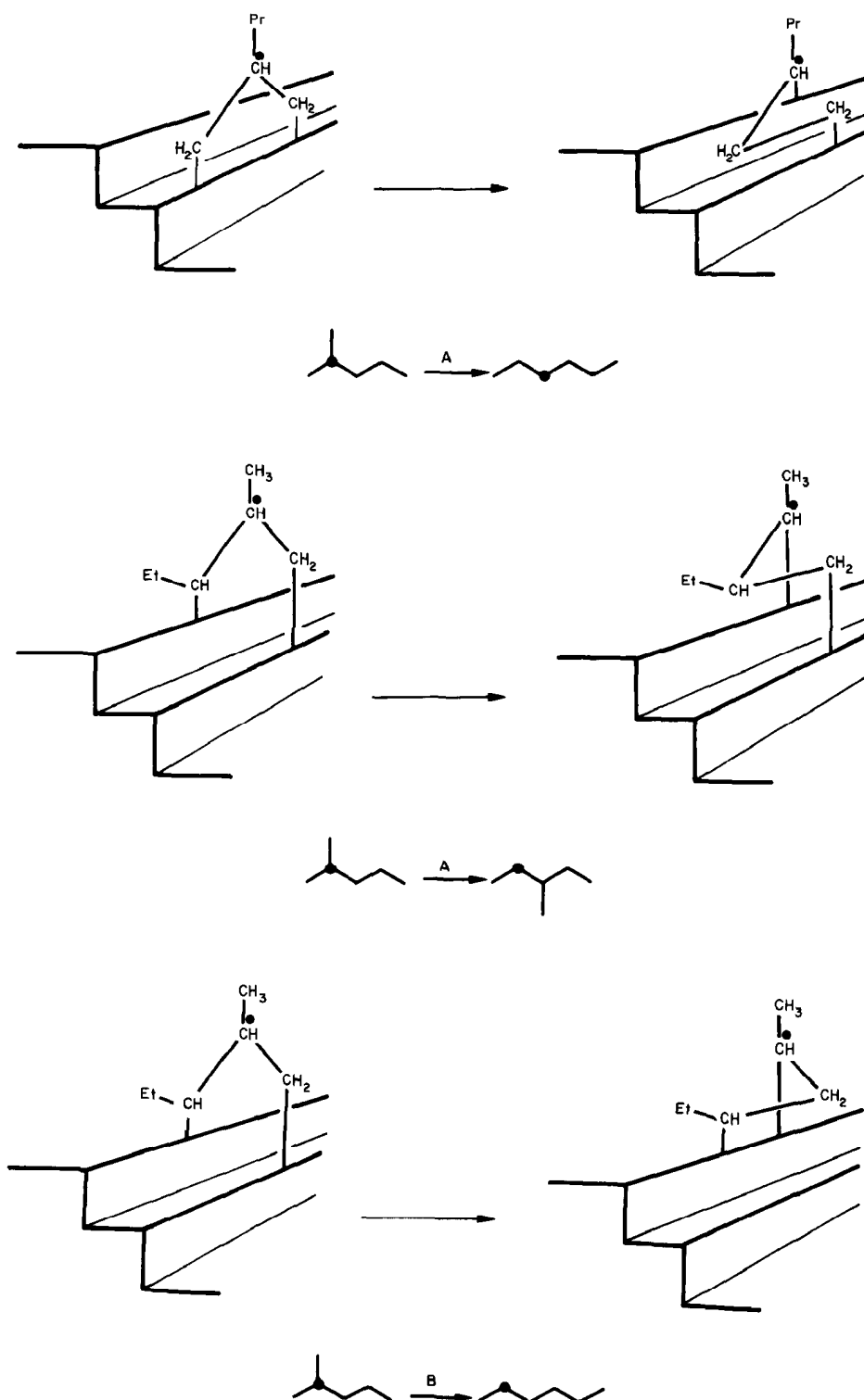


FIG. 3. Models proposed for isomerization of 2-methylpentane to 3-methylpentane or *n*-hexane via bond shift A or B on the reconstructed Pt (557) surface.

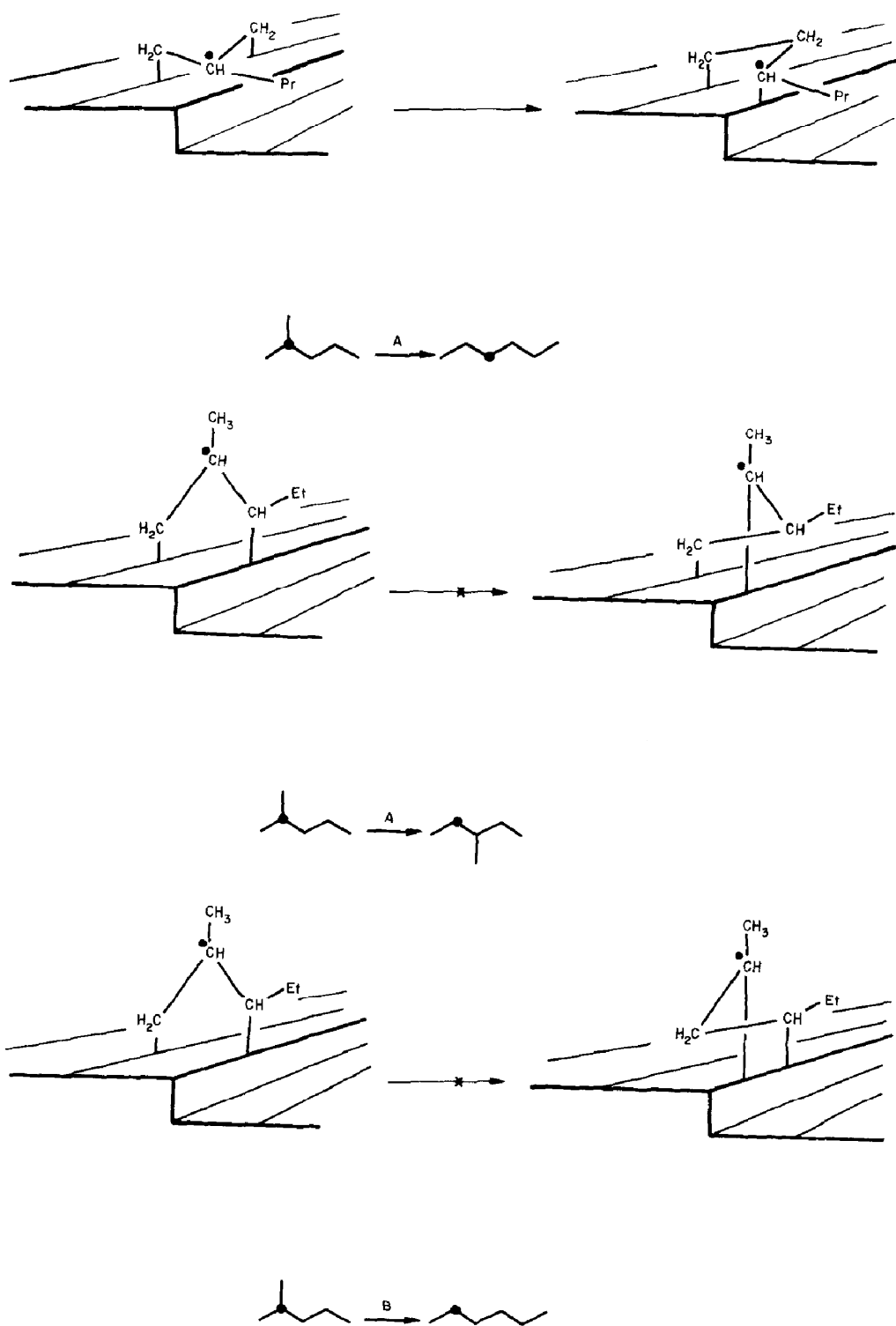


FIG. 4. Models proposed for isomerization of 2-methylpentane to 3-methylpentane or *n*-hexane via bond shift A or B on the Pt(119) surface.

face-centered cubic single crystals. They may be explained either by the presence of pseudocrystals with uncommon symmetry or, by electronic properties for the very small clusters that differ from the ones in the infinite crystals. The stepped surfaces are more active than the low index face (111). On a vicinal face of the (111) the bond shift is enhanced comparatively to a vicinal of the (100), to the (111), or to a polycrystalline foil of platinum. As shown previously by LEED, hydrogen induces step coalescence and terrace broadening on the stepped surface [ $m(111) \times (100)$ ] in the temperature range of 200 up to 500°C, which will explain the increase of bond-shift mechanism on the vicinal face of the (111). Tracer studies have shown that isomerization by bond shift (mode A) is high on the vicinals of the (111) and (100) faces. Models of adsorbed species were proposed to explain the different percentages of the bond-shift and cyclic mechanisms on the stepped surfaces studied. These models are compatible with the well-known mechanisms of skeletal rearrangements and with kinetic and energetic data obtained recently in our laboratory for isomerization, dehydrocyclization, and hydrocracking of C<sub>5</sub> hydrocarbons.

## REFERENCES

1. (a) Anderson, J. R., and Avery, N. R., *J. Catal.* **2**, 542 (1963); **5**, 446 (1966). (b) Anderson, J. R., and Baker, B. G., *Nature (London)* **187**, 937 (1960).
2. (a) Barron, Y., Maire, G., Cornet, D., and Gault, F. G., *J. Catal.* **2**, 152 (1963). (b) Barron, Y., Maire, G., Muller, J. M., and Gault, F. G., *J. Catal.* **5**, 428 (1966).
3. (a) Dartigues, J. M., Chambellan, A., Corolleur, S., Gault, F. G., Renouprez, A., Moraweck, B., Bosch Giral, P., and Dalmai-Imelik, G., *Nouv. J. Chim.* **3**, 591 (1979). (b) Gault, F. G., Garin, F., and Maire, G., in "Growth and Properties of Metal Clusters" (J. Bourdon, Ed.), p. 451. Elsevier, Amsterdam, 1980.
4. Lang, B., Joyner, R. V., and Somorjai, G. A., *Surf. Sci.* **30**, 400 (1972).
5. Blakely, D. W., and Somorjai, G. A., *J. Catal.* **42**, 181 (1976); *Nature (London)* **258**, 580 (1975).
6. (a) Kahn, D. R., Petersen, E. E., and Somorjai, G. A., *J. Catal.* **34**, 294 (1974). (b) Gillespie, W. D., Herz, R. K., Petersen, E. E., and Somorjai, G. A., *J. Catal.* **70**, 147 (1981).
7. Parayre, P., Amir-Ebrahimi, V., and Gault, F. G., *J.C.S. Faraday I* **76**, 1723 (1980).
8. Joyner, R. W., Lang, B., and Somorjai, G. A., *J. Catal.* **27**, 405 (1972).
9. Garin, F., Doctorat d'Etat (Ph.D.), Université L. Pasteur, Strasbourg (1978). Luck, F., Doctorat Spécialité, Université L. Pasteur, Strasbourg (1978). Garin, F., Luck, F., and Maire, G., unpublished results.
10. Maire, G., Plouidy, G., Prudhomme, J. C., and Gault, F. G., *J. Catal.* **4**, 556 (1965).
11. Corolleur, C., Corolleur, S., and Gault, F. G., *J. Catal.* **24**, 385 (1972); *Bull. Soc. Chim. Fr.* 842 (1969).
12. Garin, F., and Gault, F. G., *J. Amer. Chem. Soc.* **97**, 4466 (1975).
13. Gland, J. L., Baron, K., and Somorjai, G. A., *J. Catal.* **36**, 305 (1975).
14. Collins, D. M., and Spicer, W. E., *Surf. Sci.* **69**, 85 (1977).
15. (a) Ino, S., *J. Phys. Soc. Japan* **21**, 346 (1966). (b) Allpress, J. G., and Sanders, J. V., *Surf. Sci.* **7**, 1, (1967). (c) Gillet, E., and Gillet, M., *Thin Solid Films* **15**, 249 (1973).
16. Burton, J. J., *Catal. Rev. Sci. Eng.* **9**, 209 (1974).
17. Hoare, M. R., and Pal, P., *J. Crystal Growth* **17**, 77 (1972).
18. (a) Maire, G., Bernhardt, P., Legare, P., and Lindauer, G., Proc. VIIth Int. Vac. Congress and IIIrd Int. Conf. on Solid Surfaces, Sept. 1977, Vienna, p. 861. (b) Lindauer, G., Doctorat d'Etat (Ph.D.), University L. Pasteur, Strasbourg (1978).
19. Lindauer, G., and Bernasek, S. L., unpublished results.
20. Gault, F. G., *Adv. Catal.* **30**, 1 (1981).
21. Besocke, K., Krahl-Urban, B., and Wagner, H., *Surf. Sci.* **68**, 39 (1977).
22. (a) Tsang, J. W., and Falicov, L. M., *J. Phys. C (Solid State Phys.)* **9**, 51 (1976); (b) Kesmodel, L. L., and Falicov, L. M., *Solid State Commun.* **16**, 1201 (1975); (c) Tsang, J. W., and Falicov, L. M., *J. Mol. Catal.* **3**, 351 (1977-78).
23. Desjonqueres, M. C., and Cyrot-Lackmann, F., *Solid State Commun.* **18**, 1127 (1976).
24. Collins, D. M., and Spicer, W. E., *Surf. Sci.* **69**, 85 (1977).
25. Baro, A. M., and Ibach, H., *Surf. Sci.* **92**, 237 (1980).
26. Lindauer, G., Legare, P., and Maire, G., *J. Microsc. Spectrosc. Electron.* **5**, 757 (1980).
27. Lang, B., Legare, P., and Maire, G., *Surf. Sci.* **47**, 89 (1975). Carriere, B., Legare, P., and Maire, G., *J. Chim. Phys.* **71**, 355 (1977).
28. (a) Van Hardeveld, R., and Van Montfoort, A., *Surf. Sci.* **4**, 396 (1966); (b) Van Hardeveld, R., and Hartog, F., *Surf. Sci.* **15**, 189 (1969).

29. Anderson, J. R., and Avery, N. R., *J. Catal.* **7**, 315 (1967).
30. Muller, J. M., and Gault, F. G., Symposium on mechanisms and kinetics of complex catalytic reactions, Paper No. 15, Moscow (1968).
31. McKervey, M. A., Rooney, J. J., and Samman, N. G., *J. Catal.* **30**, 330 (1973).
32. Hall, L. H., and Kier, L. B., *Tetrahedron* **33**, 1953 (1977).